Dense water formation and circulation in the Barents Sea

M. Årthun[a,b,*], R. B. Ingvaldsen[c,b], L. H. Smedsrud[d,b], C. Schrum[a,b]

[a]*Geophysical Institute, University of Bergen, Bergen, Norway.*
[b]*Bjerknes Centre for Climate Research, Bergen, Norway.*
[c]*Institute of Marine Research, Bergen, Norway.*
[d]*Uni Bjerknes Centre, Bergen, Norway.*

Abstract

Dense water masses from Arctic shelf seas are an important part of the Arctic thermo-haline system. We present previously unpublished observations from shallow banks in the Barents Sea, which reveal large interannual variability in dense water temperature and salinity. To examine the formation and circulation of dense water, and the processes governing interannual variability, a regional coupled ice-ocean model is applied to the Barents Sea for the period 1948-2007. Volume and characteristics of dense water are investigated with respect to the initial autumn surface salinity, atmospheric cooling, and sea-ice growth (salt flux). In the southern Barents Sea (Spitsbergen Bank and Central Bank) dense water formation is associated with advection of Atlantic Water into the Barents Sea and corresponding variations in initial salinities and heat loss at the air-sea interface. The characteristics of the dense water on the Spitsbergen Bank and Central Bank are thus determined by the regional climate of the Barents Sea. Preconditioning is also important to dense water variability on the northern banks, and can be related to local ice melt (Great Bank) and properties of the Novaya Zemlya Coastal Current (Novaya Zemlya Bank). The dense

[*]Corresponding author. Now at: British Antarctic Survey, Natural Environment Research Council, Cambridge, UK.

Email addresses: `marius.arthun@gfi.uib.no` (M. Årthun), `randi.ingvaldsen@imr.no` (R. B. Ingvaldsen), `Lars.Smedsrud@uni.no` (L. H. Smedsrud), `Corinna.Schrum@gfi.uib.no` (C. Schrum)

water mainly exits the Barents Sea between Frans Josef Land and Novaya Zemlya, where it constitutes 63% (1.2 Sv) of the net outflow and has an average density of 1028.07 kg m^{-3}. 0.4 Sv enters the Arctic Ocean between Svalbard and Frans Josef Land. Covering 9% of the ocean area, the banks contribute with approximately 1/3 of the exported dense water. Formation on the banks is more important when the Barents Sea is in a cold state (less Atlantic Water inflow, more sea-ice). During warm periods with high throughflow more dense water is produced broadly over the shelf by general cooling of the northward flowing Atlantic Water. However, our results indicate that during extremely warm periods (1950s and late 2000s) the total export of dense water to the Arctic Ocean becomes strongly reduced.

---

1. Introduction

Dense water masses form in Arctic and Antarctic shelf seas through cooling and rejection of salt during sea-ice growth. Deep and bottom waters in the world can partly be explained by subsequent shelf convection (Killworth, 1983). In the Arctic Ocean large-scale lateral advection from the adjoining continental shelves also maintains the cold halocline layer (Aagaard et al., 1981). Hence, the brine enriched waters cascading off the continental shelves are crucial for the global ocean circulation and climate (Meincke et al., 1997).

The Barents Sea (Fig. 1) is of particular interest for several reasons. The heat transported by the Barents Sea branch of the Norwegian Atlantic Current is effectively lost through intense ocean-atmosphere heat exchange (e.g. Häkkinen and Cavalieri, 1989; Årthun and Schrum, 2010), and according to estimates based on atmospheric observations and oceanic heat budgets about half of the heat loss in the entire Nordic Seas takes place here (Simonsen and Haugan, 1996). It is also one of the largest shallow shelves ad-

jacent to the Arctic Ocean (1.4×10^6 km^2), and the deepest (230 m). The ice extent shows large seasonal variations (Kvingedal, 2005), which provides favorable conditions for ice formation and subsequent brine release. As a consequence there is seasonal formation of dense water in the Barents Sea.

Dense water formation on the shallow shelves west of Novaya Zemlya was postulated early last century by Knipowitsch (1905) and Nansen (1906). Observations confirming this were presented by Midttun (1985). Localized dense water formation is often related to opening of polynyas due to offshore winds and the influence of tides upon the ice pack (e.g. Midttun, 1985; Martin and Cavalieri, 1989; Schauer, 1995; Skogseth et al., 2004). West of Novaya Zemlya cold easterly winds during winter frequently open a polynya (Martin and Cavalieri, 1989) and more than 10 m of ice forms in this polynya during an average winter (Winsor and Björk, 2000). A recurring polynya is also known to form in Storfjorden (Fig. 1) producing 0.06-0.07 Sv (1 Sv $\equiv 10^6$ m^3 s^{-1}) of cold, dense water (often referred to as brine-enriched shelf water) during winter (Skogseth et al., 2004). The Storfjorden dense water formation is further described by e.g. Anderson et al. (1988) and Skogseth et al. (2005), and its dense outflow by e.g. Quadfasel et al. (1988) and Schauer (1995). Dense water formation in the Barents Sea has also been observed in shallow areas such as the Spitsbergen Bank, Central Bank and Great Bank (Fig. 1, e.g. Midttun, 1985; Quadfasel et al., 1992). Nansen (1906) speculated that dense water from the eastern Barents Sea could reach the Arctic Ocean through the St. Anna Trough, and this has been supported by observations (Midttun, 1985; Loeng et al., 1993; Schauer et al., 2002) and numerical models (Maslowski et al., 2004; Gammelsrød et al., 2009). Dense water formed in the western Barents Sea mainly descends into the Norwegian Sea/Fram Strait (Quadfasel et al., 1988; Blindheim, 1989; Quadfasel et al., 1992).

Earlier studies have shown that interannual to decadal variability in dense water formation is large (e.g. Midttun, 1985; Rudels and Friedrich, 2000; Schauer et al., 2002),

and potential sources of variability in dense water characteristics have been identified (e.g. Rudels, 1987; Cavalieri and Martin, 1994; Schauer, 1995; Harms, 1997; Backhaus et al., 1997; Schauer et al., 2002; Ellingsen et al., 2009). The surface salinity before the freezing season has been found to be important, but the factors controlling the salinity depend on the region being investigated. For the Novaya Zemlya Bank, freshwater carried with the Norwegian/Novaya Zemlya Coastal Current has been suggested (Rudels, 1987; Schauer, 1995; Schauer et al., 2002). Harms (1997) argued that ice freezing/melting is more important than the freshwater runoff, while Ellingsen et al. (2009) found that ice import through the northern boundaries is of major importance to dense water characteristics. Water column stability is another source of variability (Backhaus et al., 1997; Harms, 1997; Maus, 2003; Skogseth et al., 2004). According to Harms (1997) the initial stratification is dependent on the Atlantic influence on ice freezing or melting, and Backhaus et al. (1997) argued that import of warm Atlantic Water (AW) onto the Barents Sea shelf may cause a negative feedback on both deep reaching convection and ice growth. The latter is important for dense water formation through input of salt (Martin and Cavalieri, 1989; Winsor and Björk, 2000; Schauer, 1995; Skogseth et al., 2004). Furthermore, it has been recognized that as the climate of the region depends greatly on the Atlantic inflow, any variations in the characteristics of this inflow would inevitably have consequences for the production of dense water (Harms, 1997). He proposed that in a warm period high melting rates in summer and strong Atlantic inflow would tend to amplify the stratification which would reduce the bottom water formation during winter. Schauer et al. (2002) also outlined the importance of variability in AW properties due to the substantial mixing/entrainment taking place when dense water formed on the banks cascade down to deeper depressions in the Barents Sea and St. Anna Trough.

This demonstrates that in order to understand the variability in dense water formation it is necessary to investigate the large scale circulation, hydrography, forcing conditions, and
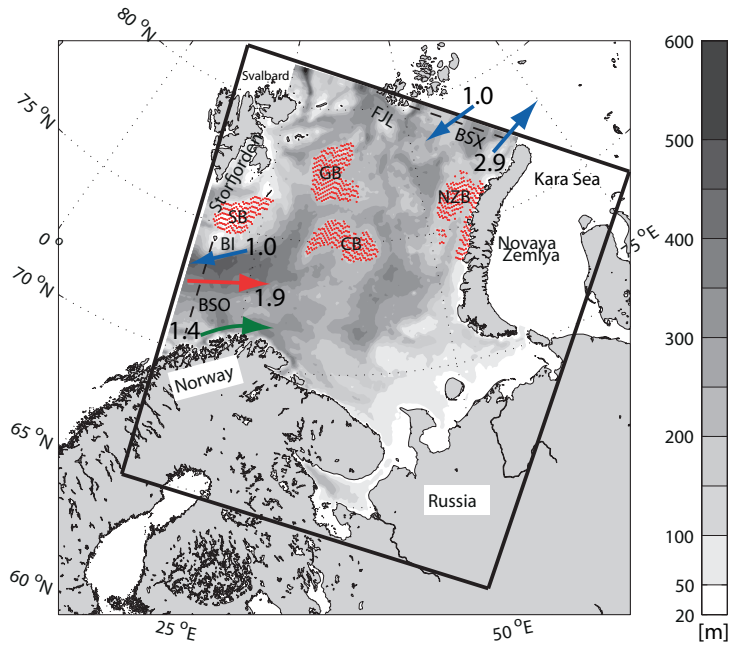
Figure 1: Model domain (black rectangle) and Barents Sea bathymetry (greyscale). The Kara Sea is not included in the model setup. Dense water formation regions highlighted in the paper are shown (details in Tab. 1). Abbreviations are SB: Spitsbergen Bank, CB: Central Bank, GB: Great Bank, NZB: Novaya Zemlya Bank, BI: Bear Island. Arrows indicate modeled major in- and outflows (mean values in Sv.) through BSO and BSX (dashed lines); the red arrow representing AW inflow ($T>3°C$, $S>35$), green arrow being mostly coastal- and surface water, while blue arrows are cold currents.

dominant mixing mechanisms preconditioning the shelf waters for dense water production. To do this we apply a new and improved setup of a regional coupled ice-ocean model to the Barents Sea for the period 1948-2007. Dense water formation and circulation on shallow banks as well as the general cooling of the AW throughflow are described, including the processes and factors involved in determining the interannual variability. In addition, we

present unpublished observations of bottom water temperature and salinity in key dense water formation areas (Spitsbergen Bank, Central Bank, Great Bank, and Novaya Zemlya Bank; Fig. 1) from 1970-2007. As earlier studies often have relied on sparse data, this makes a unique data set. We will attempt to answer the following questions:

(1) What processes are most important to dense water formation on the different banks?

(2) How does variability on the banks influence the total export of dense water into the Arctic Ocean?

(3) How does variability in the Atlantic Water throughflow influence the total export of dense water into the Arctic Ocean?

The novelty to our approach lies in that all the earlier identified sources causing variability in dense water formation are included, and so are all areas. It also lies in the resolution of temporal and regional variability in water mass transformation processes within the Barents Sea, and their influence on dense water properties on the banks and the total flow of dense water out of the Barents Sea. The Barents Sea is one of two pathways in which AW reaches the Arctic Ocean and the outflow waters are of major importance to the Arctic Ocean with respect to heat and freshwater (Gerdes and Schauer, 1997; Rudels et al., 2004; Aksenov et al., 2010), underlining the importance of water mass transformation processes in the Barents Sea. Using a multi-decadal model run in combination with an extensive set of observations we gain a better understanding of the mean state of the Barents Sea ice-ocean system, which is a prerequisite for understanding the present and future regional climate.

The paper is structured as follows: The observations and numerical model are presented in Sec. 2 together with an evaluation of the simulated mean circulation and main water masses. Dense water formation is investigated in Sec. 3 and Sec. 4. The circulation of dense water within the Barents Sea (Sec. 6) and its characteristics upon entering the

6

Arctic Ocean (Sec. 7) are also described, and variability of the outflow is discussed with respect to production on the banks compared to that produced broadly over the shelf. The main findings are summarized in Sec. 8.

2. Data and Methods

2.1. Hydrographic data

Bottom water temperature and salinity have been sampled during annual regional scientific surveys to the Barents Sea in August-October 1970-2007. Each year 4-5 Norwegian (Institute of Marine Research) and Russian (Knipovich Polar Research Institute of Marine Fisheries and Oceanography) vessels participated thus getting a regional coverage of most of the Barents Sea in a relatively synoptic manner. The hydrographic data were sampled using CTD or water bottle samples and the number of stations each year varied between 106 and 1144 with a total of more than 16500 stations over the period 1970-2007. To capture the characteristics of the dense water, the lowermost measurement from each hydrographic station was examined. If the lowermost sample was above the sea bed by more than 10% of the true depth it was rejected from the data set. The data are presented as temperature and salinity at bottom (or at the deepest observation), and we use the original samples without any interpolation.

Hydrographic data were also provided by the International Council for the Exploration of the Sea (ICES) and from the Geophysical Institute, University of Bergen (GFI-UIB). The data were processed according to Nilsen et al. (2008) and interpolated onto a $1° \times 0.5°$ grid between 18-36°E and 70-74°N. These observations are only used to evaluate the model performance in the south-western Barents Sea.

2.2. Numerical model

2.2.1. Setup

This study uses the coupled ice-ocean model HAMSOM (Hamburg Shelf Ocean Model), which has been developed at the Institute of Oceanography, University of Hamburg, Germany. The model uses non-linear primitive equations of motion, which are discretized as finite differences on an Arakawa C-grid with z-coordinates in the vertical direction. The model domain is shown in Fig. 1. The horizontal resolution is 7×7 km and the vertical dimension is resolved with 16 unevenly spaced levels with a free surface and interface boundaries at 8, 16, 24, 32, 40, 50, 75, 100, 150, 200, 250, 300, 400, 500, 600 and 700 m. The ocean model is coupled to a dynamic-thermodynamic sea-ice model. Thermodynamic ice growth is calculated following Hibler (1979), whereas the ice dynamics are based upon an viscous-plastic rheology described in Leppäranta and Zhang (1992) and Schrum and Backhaus (1999). Ice fluxes through the open boundaries are estimated by applying a zero-gradient condition normal to the boundary.

Atmospheric forcing data were obtained from NCEP/NCAR reanalysis (Kalnay et al., 1996). 6 hourly air temperatures (2 m), specific humidity (2 m), air pressure, precipitation, wind speed (10 m), and long- and shortwave radiation were applied as surface forcing. Turbulent heat fluxes (sensible and latent) were calculated by the model itself using standard bulk formula. Lateral boundary conditions for temperature and salinity were taken from the Barents and Kara Seas Oceanographic Database (BarKode, Golubev and Zuyev, 1999). A climatology from the global model C-HOPE (Marsland et al., 2003) was used in areas without sufficient observations in the northern Barents Sea. Freshwater from land is added through river runoff from four Russian rivers; Pechora, Mesen, Dvina, Onega (Lammers and Shiklomanov, 2000). Further details on the model configuration are given by Schrum and Backhaus (1999), Schrum et al. (2005) and Årthun and Schrum (2010).

The current setup differs from that described in Årthun and Schrum (2010) by the usage of new sea surface elevation and sea-ice boundary data from the Miami Isopycnic Coordinate Ocean Model (MICOM, Bleck, 1998), and the implementation of a new advection scheme. The MICOM setup from which the boundary data were generated is described in Sandø et al. (2010). The new advection scheme, a total variation diminishing (TVD) scheme, is monotonicity preserving and has very low numerical diffusion (Sweby, 1984), thus providing a better representation of fronts in temperature and salinity. Hence, the resolution of coastal currents (Norwegian Coastal Current and Novaya Zemlya Coastal Current) and the Polar Front along the Bear Island slope are improved compared to the earlier setup (Barthel et al., 2011).

The model was started from rest 01.01.1948 with temperature and salinity initial conditions from BarKode. A simulation of the year 1948 was performed twice to spin-up the model, after which the Barents Sea simulation was conducted for the period 1948-2007 using the model fields at 31.12.1948 as initial conditions.

2.2.2. Study area and model evaluation

The Barents Sea circulation is dominated by a warm inflow in the south-west and colder water masses occupying the northern areas (Fig. 2a). AW enters mainly between Norway and Bjørnøya (Bear Island), referred to as the Barents Sea Opening (BSO, Fig 1). Based on measurements from 1997-2007 the mean AW inflow is 2.0 Sv, with a maximum of 2.8 Sv in January and an April minimum of 1.1 Sv (Smedsrud et al., 2010). Higher inflow during winter is related to stronger winds due to passing atmospheric lows (Ingvaldsen et al., 2002). Closer to the Norwegian coast, the colder and fresher Norwegian Coastal Current provides an additional 1.1 Sv (Skagseth et al., 2011). A fraction of the AW recirculates within the Bear Island Trough and together with the cold Bear Island Current forms a bottom intensified westward flow of 0.9 Sv (Skagseth, 2008). Consider-

ing the entire water column yields a mean heat transport into the Barents Sea of 49±7 TW (Skagseth, 2008). However, the heat transport from the Norwegian Coastal Current has not been well quantified, and new calculations based on measurements suggest that the contribution from the coastal current may be as much as 34 TW (Skagseth et al., 2011), increasing the net heat transport by ~50%. Following Gammelsrød et al. (2009), the out-flow between Frans Josef Land and Novaya Zemlya (denoted Barents Sea Exit, BSX) for 1991-1992 is 2.2 Sv, including Cold Bottom Water (1.0 Sv), Arctic Water (0.4 Sv), AW (0.2 Sv), Surface Water (0.1 Sv), and 0.5 Sv of remaining unspecified water types. Hence, cold, dense water is one of the principal contributors to the outflow.

The model captures the principal features of the hydrographic structure in the Barents Sea (Fig. 2a), and the model mean temperature distribution (0-200 m) during February 1981-2004 compare well with observations (ICES/GFI-UIB; filled circles). Based on these observations an annual time series was also constructed for the period 1975-2004 (not shown). The interannual variability is reproduced by the model when compared to annual mean temperatures between 0-200 m; the correlation coefficient (r) being 0.91. The mean observed temperature (T) is 5.05°C, while the simulated mean temperature is 4.97°C. For the simulated salinity (S) the correlation is 0.66 with a small bias (0.07) towards higher values. The interannual variability in integrated sea-ice area is also captured by the model (Fig. 2b) compared to satellite derived data from the National Snow and Ice Data Center (Cavalieri et al., 1996).

The modeled annual mean net inflow through BSO is 2.3 Sv (Fig. 1), with higher/lower inflow during winter/summer (not shown). The inflow to the Barents Sea through this section is 3.3 Sv dominated by 1.9 Sv of AW ($T > 3$°C and $S > 35$). The rest of the inflow (1.4 Sv) consists of fresher water ($S < 34.5$) flowing along the Norwegian coast and surface
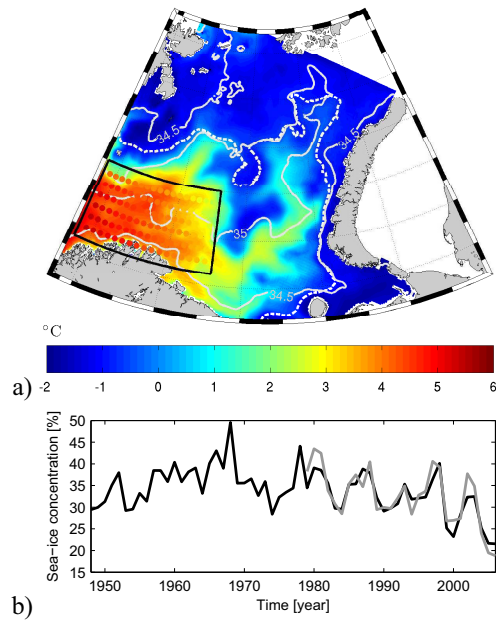
Figure 2: a) Mean simulated temperature (color) and salinity (gray lines) during February 1981-2004 over 0-200 m depth. Only 34.5 and 35 salinity contours are shown to mark coastal waters and AW. The black box indicates the area from where time series were extracted. Observations interpolated onto a 1°×0.5° grid are shown as colored circles. The February mean ice edge (concentration: 30%) is also included, indicated by the dashed white line. b) Winter mean (November-April) sea-ice concentration from HAMSOM (black) and from satellite data (SMMR/SSMI) between 70-81°N and 15-60°E.

water. The simulated net heat transport[1] into the Barents Sea of 60 TW is within the range of previous estimates, e.g. Zhang and Zhang (2001, 43 TW), Aksenov et al. (2010, 60

---

[1]Heat transport is calculated the traditional way using the simulated temperature, velocity, heat capacity and water density (see e.g. Årthun and Schrum, 2010). Calculations are relative to -0.1°C in order to compare with cited literature.

11

TW) and Sandø et al. (2010, 74 TW). The simulated flow through BSX also compares well with the observations from Gammelsrød et al. (2009).

3. Dense water characteristics

Based on observations of dense water formation in the Barents Sea (e.g. Midttun, 1985; Quadfasel et al., 1992) areas of special interest were defined (Fig. 1 and Tab. 1), and time series of observed and modeled dense water properties were constructed. Although the observations are from late summer, they have signatures of dense water produced during the previous winter because remnants are trapped on the shelves over summer (Midttun, 1985; Ivanov et al., 2004). Using theory and observations to investigate cascading events Shapiro et al. (2003) found that the estimated time for a dense water body to sink from the Novaya Zemlya Bank would be 7 months, and the later stages of winter cascading can therefore be observed the following summer. Identifying the dense water characteristics by using vertical integrated values over the water column and over a specific temperature-salinity domain would give more robust calculations. Unfortunately this can not be done due to low and irregular vertical resolution in the historical data, and thus motivates and necessitates the use of a numerical model. The strength of a modeling based approach is that it allows for integration on a regular grid over a long period and hence accounts for variability on different time and spatial scales. Thus, it minimizes errors from undersampling, in contrast to observational based investigations which can be subject to strong undersampling errors. This is especially the case for wintertime processes in Polar Regions, such as dense water formation.

3.1. Observed bottom water

The observed bottom water characteristics from Central Bank and Novaya Zemlya Bank are shown in Fig. 3. The *T-S* properties on Central Bank show high salinities

Table 1: Data selection criteria for dense water formation regions.

Region	Lat. [°N]	Lon. [°E]	Depth [m]	A [10^4km^2]	V [10^{12}m^3]
Spitsbergen Bank	74.8-76.5	18-27	<100	2.5	1.8
Central Bank	74.3-76	32-44	<200	3.1	6.2
Great Bank	76.25-78.8	32-40	<200	3.6	6.6
Novaya Zemlya Bank	73.8-77	51.2-60	<150	3.2	4.0

(S>34.75) and a narrow salinity range, but span a wide range (4°C) in temperature. There is also a (weak) indication that high salinity corresponds to high temperature. All of these factors indicate that AW constitutes a major fraction of the bottom water. Due to the high salinity of AW cooling alone is sufficient for densification of the surface waters, and only minor signatures of freezing are evident. Mean bottom density on Central Bank based on observations is 1028.1 kg m^{-3}. On Novaya Zemlya Bank on the other hand, there are numerous observations along the freezing line, and high salinity clearly corresponds to low temperature. Densification by brine release is thus a common process in this area, as previously noted by e.g. Midttun (1985). T-S properties are still variable, probably reflecting both strong exchange since winter and influence of coastal water and modified AW intruding on the bank. Due to the lower salinities the mean density on Novaya Zemlya Bank (1028.0 kg m^{-3}) is lower than on Central Bank.

Corresponding time series reveal large temporal variability in bottom water hydrography (Fig. 4). On the Spitsbergen Bank the temperature range from -0.1°C in 1975 to 5.0°C in 2006, while the salinity range is 1.07. The Central Bank has the most saline bottom water (34.93) and displays less variability, particularly in salinity. The Great Bank also has a narrow range in salinity (0.29), whereas temperatures vary from -0.9°C to 1.2°C. The coldest water is found on Novaya Zemlya Bank with an average temperature of -1.2°C. The average salinity is 34.87.
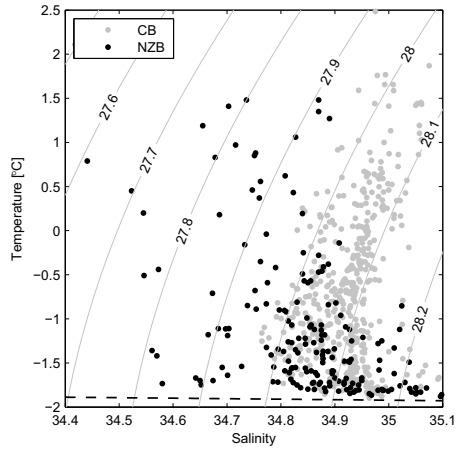
13

Figure 3: Temperature-salinity diagram of observed bottom water on the Central Bank (CB) and Novaya Zemlya Bank (NZB) between 1970 and 2007. Dashed line shows the freezing point temperature.

3.2. Simulated bottom water

The simulated bottom water temperature and salinity are also included in Fig. 4. Compared to the observed variability on the banks (indicated by the standard deviations) Spitsbergen Bank is well represented in the model. The other banks tend to be biased compared to observations. It should, however, be recognized that the model data are 3-month averages (August-October), which are being compared to irregular observations in both time and space. The limited amount of observations implies that local spatial variability may not be resolved. Hydrography on Spitsbergen Bank and Great Bank are strongly influenced by the south-westward flowing Persey Current/Bear Island Current and East Spitsbergen Current (Loeng, 1991; Maslowski et al., 2004), whose properties are affected by the inflow between Svalbard and Frans Josef Land. The northern inflow consists mainly of cold and fresh Arctic type waters, but also a branch of AW (Mosby, 1938; Pfirman et al., 1994). In the northern Barents Sea this is a subsurface water mass, underlying the colder, less
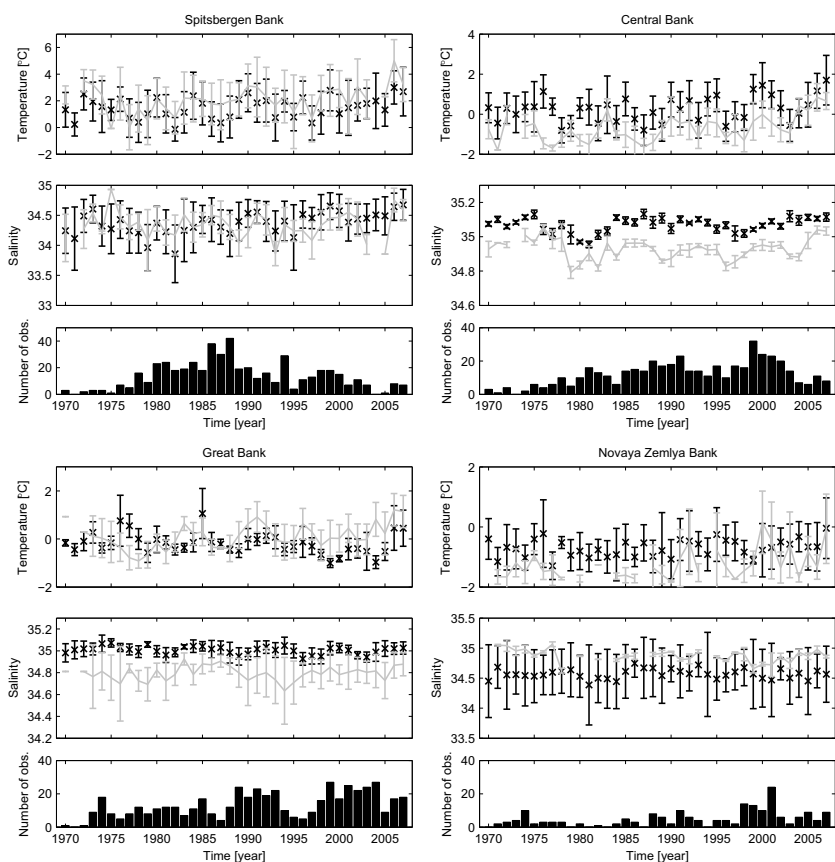
14

Figure 4: August-October averages and standard deviation of simulated (crosses) and observed (gray line) bottom water temperature and salinity between 1970 and 2007. The annual data coverage is also included. Note the different scales. Observed standard deviations were calculated based on all available data from individual years, whereas the simulated standard deviations are based on August-October averages from all model gridpoints within the specific domains (Tab. 1).

saline water. Due to lack of observations no temperature or salinity anomalies are pre-

scribed at the northern open boundary to account for interannual variability in water mass properties. Boundary values are also partly based on model climatology. Not resolved variability in the characteristics of inflowing water in the north-western Barents Sea, and hence the stratification, can therefore partly explain the colder simulated bottom water on Great Bank. Potentially overestimated vertical mixing as a result of weak stratification will also influence bottom water properties in this area (e.g. the higher simulated salinities on Great Bank).

On Novaya Zemlya Bank the simulated bottom water temperature and salinity are biased too high and too low, respectively. From Fig. 1 and Fig. 2 it is seen that Novaya Zemlya Bank is located at the boundary between the fresh Novaya Zemlya Coastal Current and the warmer, more saline West Novaya Zemlya Current, indicated by the 34.5 isohaline. Across the frontal zone salinity varies by more than 1 (Ivanov and Shapiro, 2005). The salinity on Novaya Zemlya Bank is thus sensitive to both the position of the front and place of measurement. Considering only years with more than 10 observations on Novaya Zemlya Bank results in a much reduced bias.

The Central Bank is located close to the position of the Polar Front, which separates AW in the south from Arctic Water in the north (Loeng, 1991). Warmer and more saline bottom water thus indicates excessive AW influence in the model. This can be related to the properties and strength of the BSO inflow, but also underestimated mixing between the subsurface AW and overlying Arctic Water. The latter is discussed with respect to turbulence closure schemes and horizontal resolution in Sundfjord et al. (2008). Furthermore, deficiencies in atmospheric forcing data exist, including underestimation of NCEP surface wind speeds (Smith et al., 2001) and, hence, ocean mixing.

Consequently, a direct comparison is not straightforward and one can not expect the model averages to match observed snapshots obtained over typically shorter periods. The observed and simulated time series still display similar interannual variability; correlation

16

coefficients between simulated and observed temperature and salinity time series being significant for all locations except Great Bank. Together with the presented model evaluation (Sec. 2.2.2) this gives confidence in the general model performance and that the model provides adequate skill to investigate dense water variability on interannual timescales, although there is a bias in the simulated bottom water characteristics. Previous studies (Harms et al., 2005; Schrum et al., 2005) also concluded that HAMSOM is suitable to study climatic variability of water mass transformation processes in the Barents Sea.

3.3. Cold Deep Water

To utilize the vertical resolution of the model results, we hereafter define dense water by $T<0°C$ and $S>34.75$. This corresponds to densities above 1027.9 kg m^{-3}, and is referred to as Cold Deep Water (CDW).

Time series of simulated winter mean (November-April) CDW temperature, salinity and the corresponding density from the banks show pronounced interannual variability (Fig. 5). Salinities above 35 are found on all banks. The average salinity is highest on Central Bank (35.00), whereas the highest monthly mean salinities are found on Spitsbergen Bank and Novaya Zemlya Bank, being 35.30 and 35.31, respectively. These banks are also associated with the lowest average temperatures (T=-1.3/-0.8°C). Significant (negative) correlation is found between temperature and salinity on Novaya Zemlya Bank, indicative of ice growth and salt input. At the end of winter (April) the average integrated volume of CDW varies from $6 \cdot 10^{11}$ m^3 on Spitsbergen Bank to $38 \cdot 10^{11}$ m^3 on Central Bank. Assuming that all the CDW is formed locally during winter this amounts to a winter average of 0.04 (Spitsbergen Bank), 0.24 (Central Bank), 0.21 (Great Bank), and 0.06 Sv (Novaya Zemlya Bank), respectively (Fig. 5). These values are similar to the amount produced in the Storfjorden polynya (Skogseth et al., 2004) and in Arctic polynyas (Cavalieri and Martin, 1994; Winsor and Björk, 2000). On Central Bank and Great Bank the vol-
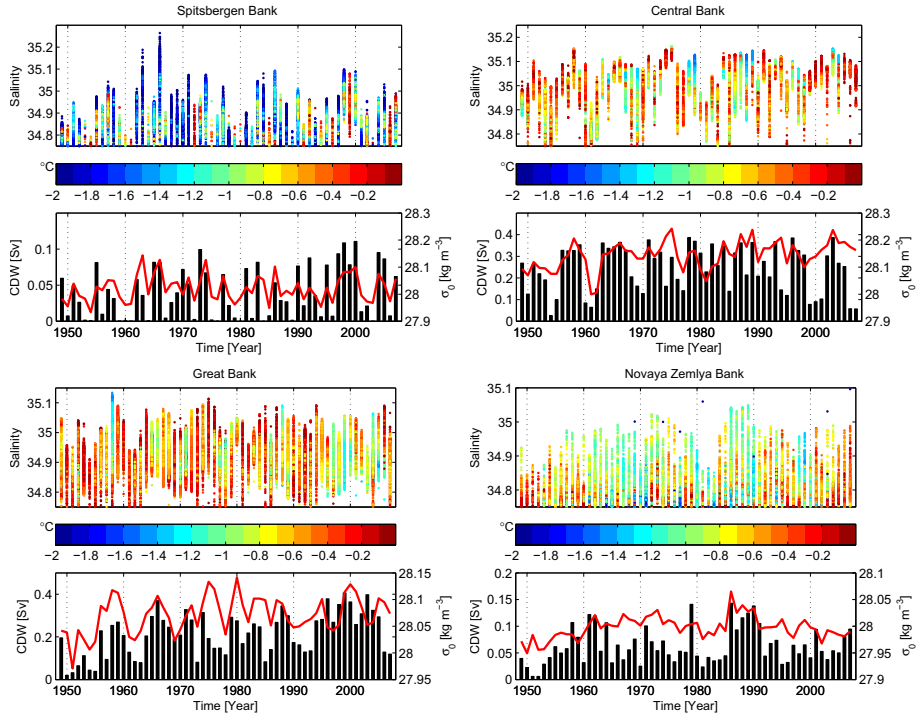
17

Figure 5: Upper: Simulated winter mean (November-April) CDW ($T<0°C$ and $S>34.75$) temperatures (colorscale) and salinities between 1948 and 2007. Lower: CDW volume flux and density (red line) during winter. Fluxes are estimated based on April mean CDW volume.

ume and density of the CDW are positively correlated ($r=0.71$ and $r=0.55$, respectively). Thus, during periods of high formation the CDW is also denser. This is not the case for Spitsbergen Bank and Novaya Zemlya Bank where the correlation between volume and density is not significant. The total contribution from the banks (0.55 Sv) is influenced by quasi-regular fluctuations with periods of about 5-8 years, in agreement with observed variability in the Barents Sea climate (warm/cold periods; Ingvaldsen et al., 2003). This

will be elaborated on in Sec. 5 and Sec. 7.

4. Dense water formation processes and regional variability

Variability in properties and amount of CDW on the banks are governed by the combination of initial conditions, atmospheric forcing (oceanic heat loss) and ice production. The following results and discussion identify and address the differences in these processes among the different banks. Local forcing such as tides may influence CDW formation through redistribution of sea-ice and, hence, increased ice production, and will also be discussed.

4.1. Initial salinity - Preconditioning

CDW formation is driven from the surface, and the initial surface salinity is important for the volume formed during winter. With low initial salinity more salt must be rejected for the surface water to become sufficiently saline for CDW. To investigate the sensitivity of the different banks to this preconditioning parameter, the simulated surface salinity anomalies in November (S_0) are displayed in Fig. 6 and compared to salinities in April (S_1). Highest initial salinities are found on Central Bank (34.71), which also has the lowest salinity increase during winter ($\Delta S = S_1 - S_0$). Lowest mean initial salinities are found on Great Bank (33.13), but this bank has the highest interannual variability (range=2.5) and the largest surface salinity increase during winter (1.1). Great Bank also shows a clear increase in initial salinities during the last decades, which is reflected in the amount of CDW (Fig. 5). Spitsbergen Bank, Central Bank and Great Bank show a positive correlation ($r \sim 0.6$) between November and April salinities. Positive correlation indicates that variations in initial salinity are more important for the April salinities than variations in local ice growth and salt rejection. Thus on these banks the initial salinity is an important preconditioning factor for CDW formation during winter, and significant correlation

19

to CDW volume is found (r=0.35-0.44). On Novaya Zemlya Bank there is no statistical significant correlation between November and April salinities, although it is important to the maximum salinity reached during winter (not shown). CDW formation is also less sensitive to the initial salinity (r=0.27).

Low initial salinity also tends to give a stable water column in fall. This can cause early ice formation and brine rejection (Rudels, 1987), but normally inhibit CDW formation (Harms, 1997). The importance of stratification is evaluated by correlation between the initial surface salinity and the salinity increase during winter (ΔS). Strong negative correlations (r~-0.9) are found on Central Bank and Novaya Zemlya Bank. On these banks the stratification associated with low initial salinity can increase the brine rejection, but the stratification is still strong enough to prevent deep-reaching convection.

The above results indicate that on Spitsbergen Bank and Great Bank the initial salinity is important mostly because low initial salinity requires higher salt input for the surface water to become CDW. On Central Bank and Novaya Zemlya Bank on the other hand, the initial salinity is most important through its effect on the stratification.

4.2. Atmospheric cooling

Oceanic heat loss contributes to CDW formation by cooling the inflowing AW and lowering the temperature in the northern Barents Sea to the freezing point, initiating ice growth. In the Barents Sea oceanic heat loss to the atmosphere is high and the northeastward flowing water is cooled considerably before it enters the Arctic Ocean (e.g. Simonsen and Haugan, 1996; Schauer et al., 2002). Of the four regions Central Bank experiences the strongest atmospheric cooling with a simulated winter mean/max heat loss of 143/215 W m^{-2}, which will cool the upper 100 m by ~4.5/7°C. The mean heat loss on Spitsbergen Bank, Great Bank and Novaya Zemlya Bank is 91, 44, and 108 W m^{-2}, respectively. Spitsbergen Bank and Central Bank have positive correlations between the
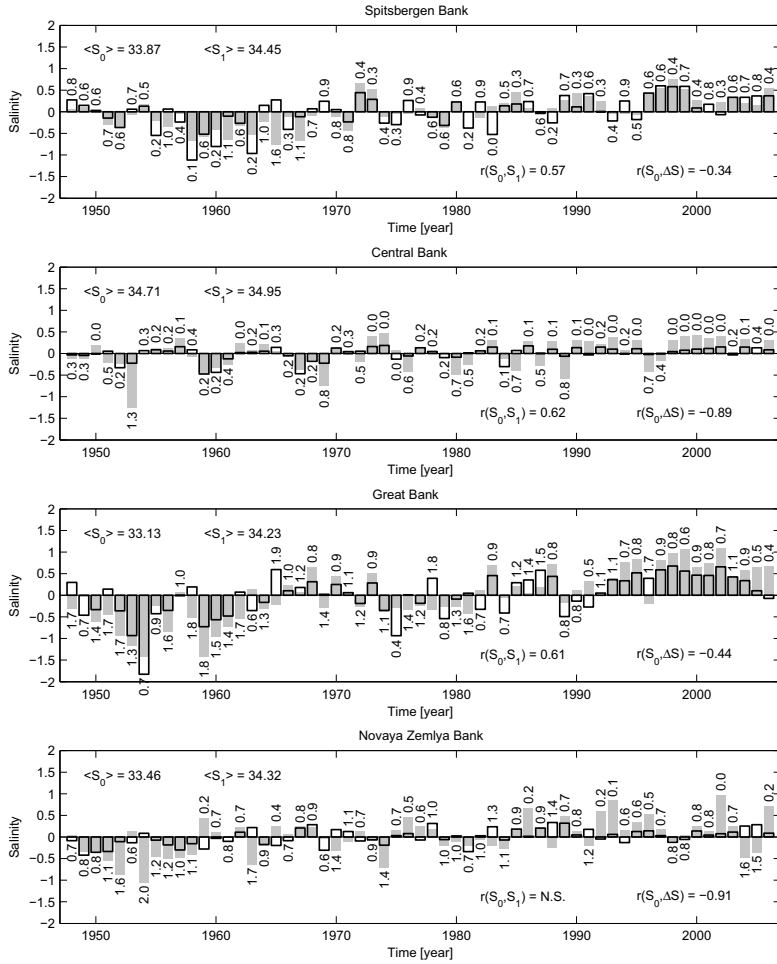
Figure 6: Simulated surface initial- (November (S_0); gray bar) and spring (April (S_1); open bar) salinity anomalies relative to respective mean values ($<S_0>$,$<S_1>$). Numbers next to the bars indicate the salinity increase during the freezing season (ΔS). Correlation coefficients between S_0 and S_1, and S_0 and ΔS are also displayed. N.S. indicate not significant at 95% confidence level.

local heat flux and the volume of CDW formed during winter; $r=0.60$ and $r=0.53$, respectively. On Great Bank and Novaya Zemlya Bank the correlation between heat flux and CDW volume is not statistically significant indicating that other processes are more dominant for the variability. For more details on the air-sea heat exchange in the Barents Sea we refer to recent works by Sandø et al. (2010), Smedsrud et al. (2010), and Årthun and Schrum (2010).

4.3. Sea-ice formation and salt fluxes

Accumulated salt release during winter from sea-ice growth and the associated water column salinity increase are shown in Fig. 7. Salt input is on average highest on Novaya Zemlya Bank ($1 \cdot 10^{12}$ kg ~ 0.2 kg m^{-2} day^{-1}), and the simulated salt flux from this bank agrees with estimates from Martin and Cavalieri (1989) based on open water regions (polynyas) along the west coast of Novaya Zemlya. Largest variability is found on Central Bank which may be almost completely ice free during some winters. Thermodynamic ice growth is not part of the model output and can not be estimated directly. The modeled mean April ice thicknesses, however, vary from 0.2 m on Central Bank to 1.5 m on Great Bank, which concurs with estimates of local first-year ice growth in the Barents Sea (Vinje, 2009).

Without water exchange, the total released mass of salt is able to increase the overall salinity on Spitsbergen Bank by up to ~0.5 and by ~0.3 on Novaya Zemlya Bank (Fig. 7). Due to greater depths (Tab. 1) the salinity increase is smaller on Central Bank and Great Bank and a stronger salt input is needed for increasing the CDW volume on these banks. However, only Central Bank has a positive correlation between salt input and CDW volume ($r=0.45$). Salt input anomalies are often opposite to surface salinities and heat loss. On Spitsbergen Bank and Central Bank this points to the influence of AW, with higher AW inflow leading to higher sea surface temperature and salinity, less ice,

and higher heat loss (e.g. Ådlandsvik and Loeng, 1991). Less ice also implies a higher surface salinity the following year due to less ice melt. The connection between dense water (CDW) formation and regional climate variability is further discussed in Sec. 5.
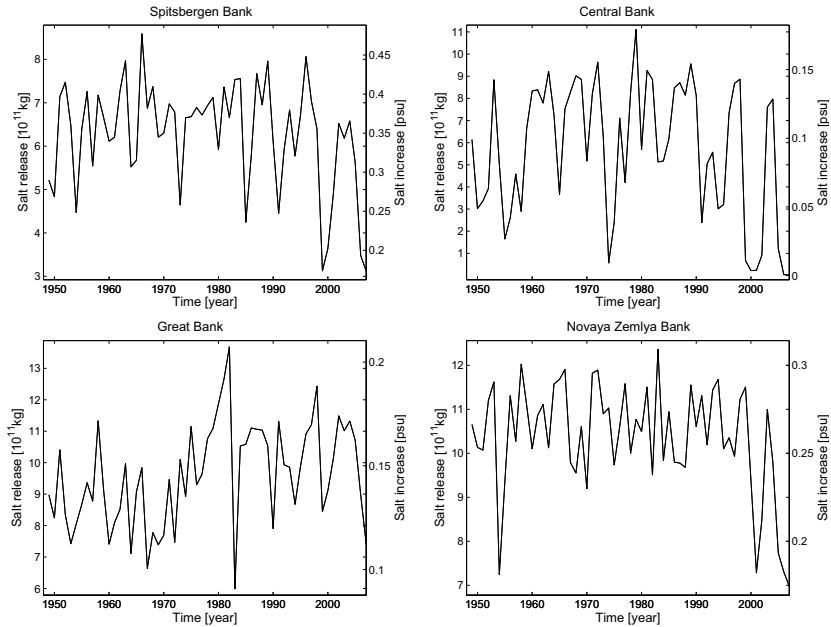

Figure 7: Released mass of salt from ice growth during winter (left axis) and corresponding salinity increase in entire water column using the mean depth on each bank.

4.4. Wind and tidal forcing

Winds and tides act to create motion in the ice pack (divergence, convergence and ridging), which influences the open water area and thus the air-sea heat exchange and ice production under freezing conditions (Kowalik and Proshutinsky, 1994). Tides also influence the temperature and salinity distribution in the Barents Sea due to increased

mixing and changes in the mean current structure (Parsons, 1995). In the Barents Sea areas of strong tidal currents are found north of Bear Island (close to Spitsbergen Bank) and near the entrance to the White Sea (Padman and Erofeeva, 2004). The semidiurnal lunar tide (M_2) is included in HAMSOM. This is the dominant tidal constituent in the Arctic Ocean and surrounding shelf seas, accounting for 79% of the tidal potential energy (Padman and Erofeeva, 2004). The prescribed tidal solution has earlier been evaluated in terms of amplitude and phase and agreed well with observations and tidal models (Harms et al., 2005).

To investigate the impact of tides the model was run without tides for the period 1979 to 1984, which corresponds to a period with average ice extent (Fig. 2b). On Spitsbergen Bank including tides increases the winter mean open water fraction by 7%. This leads to 14 W m^{-2} additional heat loss (not shown), and the corresponding additional ice growth increases the salt rejection by ~3% ($2 \cdot 10^{10}$ kg). During some months the tidal induced heat loss is >30 W m^{-2} causing a decrease in ice concentration by 10-15%, which is comparable to values obtained in the Weddell Sea (Koentopp et al., 2005). Central Bank and Novaya Zemlya Bank also show a reduced sea-ice cover during winter (~5%) and similar heat flux anomalies due to tides. No response in terms of salt input is visible, in agreement with Kowalik and Proshutinsky (1994). Ice divergence and salt rejection on Novaya Zemlya Bank are seemingly more wind related. During winter the dominant surface winds along the northwest coast of Novaya Zemlya are from east/south-east (NCEP data, not shown), which is favorable for polynya activity and localized sea-ice formation (Martin and Cavalieri, 1989). It is, however, the strength of the alongshelf (rotated coordinate system) wind component which is most important for the simulated ice growth variability (r=-0.46). This is probably related to Ekman drift which pushes the ice away from the coast during northerly winds.

4.5. CDW sensitivity to temperature and salinity classification

The choice of CDW definition is, although based on previous studies in the Barents Sea (e.g. Gammelsrød et al., 2009), somewhat arbitrary. Water mass characteristics are also slightly different in the model compared to the bottom water observations (Fig. 4). To evaluate to what extent this influences estimates of CDW volume the model mean error (bias) at the respective regions was calculated and the CDW definition adjusted accordingly (e.g. S_{CDW}>34.89 on Central Bank based on simulated values being 0.14 higher than observations). In total this does not change the CDW volume estimate noteworthy. The combined contribution from Great Bank and Novaya Zemlya Bank remains close to constant; the respective values being 0.08 Sv and 0.18 Sv compared to 0.21 Sv and 0.06 Sv in the previous calculation. CDW formation on Central Bank increases from 0.24 to 0.32 Sv and remains low on Spitsbergen Bank (0.03 Sv). On Spitsbergen Bank and Novaya Zemlya Bank the sensitivity in CDW volume is mostly due to changes in the salinity criteria for CDW, whereas Central Bank and Great Bank estimates are more influenced by the temperature limit. The interannual variability in CDW volume on each bank is nearly independent of water mass definition, and our discussion on CDW variability remains valid.

5. Sensitivity to regional climate variability

The Barents Sea climate is known to fluctuate between a warm and a cold state with periods from 3-4 years to several decades (Ådlandsvik and Loeng, 1991; Ingvaldsen et al., 2003; Levitus et al., 2009). Cold periods are characterized by extensive ice cover (Fig. 2b, Vinje, 2009) and low surface salinities due to ice melt (Maus, 2003). Warm periods are characterized by higher salinities, less ice (short freezing season) and higher air-sea heat fluxes (Årthun and Schrum, 2010). To evaluate the sensitivity of the different banks to

Table 2: Correlation coefficients and time lags (@years) between properties of the inflow between Norway and Bear Island ($BSO_{t,s}$), CDW temperature and salinity in April ($CDW_{t,s}$), Barents Sea ice extent (I_w), initial salinity (S_0), and salt input due to ice formation (S_i). Time series of ice extent and inflow are July-June averages. N.S: Not significant at the 95% confidence level based on the Student t-test.

Region	BSO_t-CDW_t	BSO_s-CDW_s	BSO_s-S_0	I_w-CDW_t	I_w-CDW_s	I_w-S_0	I_w-S_i
Spitsbergen Bank	N.S	0.31	0.41	N.S	N.S	-0.27@1	0.44
Central Bank	0.62	0.63@2	0.31@1	-0.63	N.S	-0.29@1	0.63
Great Bank	N.S	N.S	0.28@1	N.S	N.S	N.S	N.S
Novaya Zemlya Bank	0.52@1	N.S	N.S	-0.54	0.30	N.S	0.50

regional climate variability, CDW characteristics are compared to properties of the BSO inflow and the integrated ice extent (Tab. 2) which are good indicators of the climatic state of the area (e.g. Ådlandsvik and Loeng, 1991; Sandø et al., 2010).

On Spitsbergen Bank and Central Bank the properties of CDW are closely linked to the inflow characteristics through BSO and corresponding heat loss at the air-sea interface. Their location near the mean ice edge also makes them sensitive to fluctuations in regional ice extent, affecting both the surface preconditioning and CDW temperature and salinity. Low initial surface salinities coincide with periods with an extensive ice cover the previous spring and a fresher inflow (less AW) through BSO. Thus on these southern banks the CDW production is closely linked to the regional climate of the Barents Sea.

On Great Bank the CDW variability can not be related to any of the regional climate indicators used here (Tab. 2) except for salinity anomalies from BSO which influence the surface salinity. The more localized variability in the north-western Barents Sea is supported by an empirical orthogonal function (EOF) analysis of monthly sea-ice concentrations (Fig. 8). The dominant mode of variability reflects the fluctuations in the ice edge and in the north-eastern Barents Sea, whereas the second mode has the largest amplitudes in the north-west and accounts for >40% of the local variance on Great Bank. The pattern of the second mode also suggests that ice transport between Svalbard and Frans Josef

Land is of importance to Great Bank ice variability. A comparison between winter ice concentration on Great Bank and simulated ice transport yields significant co-variability. Stronger ice import causes more ice melt locally and consequently lower initial salinity the following year. The CDW variability on Great Bank is thus more affected by ice import from the north than regional climate indicators. Ice import and the associated freshwater input have been found by earlier studies to have a large influence on salinity anomalies in the Barents Sea (Maus, 2003; Ellingsen et al., 2009), and to contribute to the stronger stratification in the northern Barents Sea which is important to water mass transformations (Steele et al., 1995; Harms, 1997). The most dominant signal in the the initial salinity on Great Bank is the long term increase over almost the entire simulation period (Fig. 6). Such a trend is also visible, but less dominant on the other banks. Higher surface salinities are consistent with the observed decline in sea-ice extent, due in large part to increasing sea surface temperatures and southerly winds (Francis and Hunter, 2007). A trend in outflow of Arctic Ocean sea-ice into the Barents Sea has not been observed (Kwok, 2009).
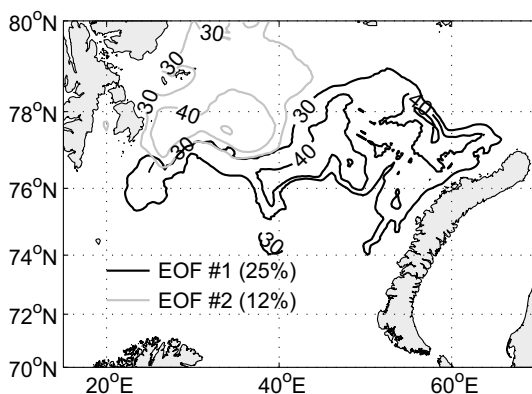

Figure 8: Local explained variance of monthly sea-ice concentration by EOF #1 and #2. Contour interval is 10%. See e.g. Schrum et al. (2006) for description of the statistical method.

On Novaya Zemlya Bank local ice growth is reflected in the regional ice extent, which affects the temperature and salinity (Tab. 2) and therefore the density of CDW. Surface salinity variability is, on the other hand, not captured by regional variability. The freshwater content west of Novaya Zemlya is affected by the characteristics of the Novaya Zemlya Coastal Current (Schauer et al., 2002). Fig. 9 shows how the freshwater input in the southern Barents Sea is advected east and north toward Novaya Zemlya Bank during winter. Highest correlation coefficients in the Pechora Sea indicate that freshwater from the major Russian rivers (model input from R-ArcticNET; Lammers and Shiklomanov, 2000) is highly important, although the freshwater transport by the Norwegian/Murmansk Coastal Current may also contribute. The simulated mean northward freshwater transport west of Novaya Zemlya (section depicted in Fig. 9) is 6.9 mSv for a reference salinity of 34.8. Higher freshwater fluxes are associated with lower initial salinities and less CDW formation on Novaya Zemlya Bank. The importance of the freshwater carried by the coastal currents to the thermohaline conditions and dense water cascades west of Novaya Zemlya was examined by Ivanov and Shapiro (2005), and was also suggested by Rudels (1987) to be the cause of the early ice formation and brine rejection in this area.

6. Cold Deep Water circulation

To investigate the circulation of CDW within the Barents Sea and toward the Arctic Ocean, an Eulerian advection model, which utilizes the simulated daily transport fields from HAMSOM, is used. The bottom layer of the selected regions was filled with a passive tracer. The tracer was then released as a pulse and transported and diffused by the simulated transports and vertical turbulence, enabling tracking of the individual paths. In Fig. 10 the tracer concentrations are shown for the initial state, taken as April 1, 2000, and then after 3 months (July 1) and 7 months (November 1). The main paths of CDW from the different banks at the given dates are indicated with arrows.
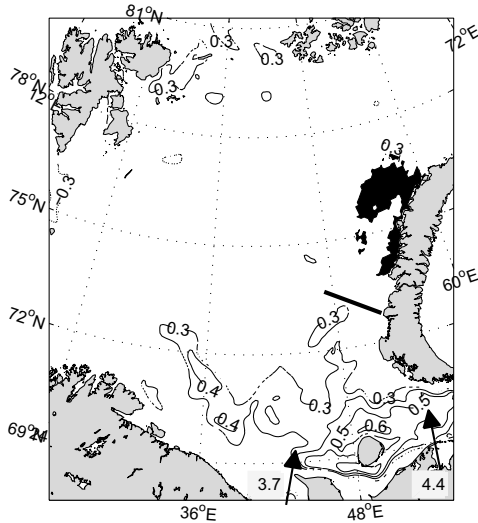
28

Figure 9: Lagged correlation between surface initial salinity (November) and Novaya Zemlya Bank salinity in April. The bank area is shaded black (Tab. 1). Isolines are drawn for significant (95%) correlations, and contour interval is 0.1. Numbers in gray boxes are annual mean river runoff from Pechora (4.4 mSv) and Dvina/Mezen/Onega (3.7 mSv), arrows indicate location of the rivers, and the solid black line indicates the section used for freshwater flux calculation.

We first focus on the waters leaving in the BSX, which include CDW formed on Central Bank, Great Bank and Novaya Zemlya Bank (Fig. 10). The Novaya Zemlya Bank is closest to the BSX and the water has the most direct path out of the Barents Sea. The CDW is thus less influenced by along-path mixing, and contributing to the densest fraction in BSX and St. Anna Trough despite having smaller volume and lower density than the two other banks (Fig. 5). Some water from this bank is also seen to flow west into the Northeast Basin and the Novaya Zemlya Canyon. This agrees with correlations between observed bottom salinity on the bank and horizontal fields of bottom salinity (not shown).

29

Midttun (1985) and Schauer et al. (2002) also observed dense water from the bank area spreading west into the deeper depressions of the eastern Barents Sea. The westward flow is more pronounced if the simulation is performed for 1979 (time of survey in Midttun, 1985), a year with lower inflow through BSO and corresponding northward flow along Novaya Zemlya. However, in neither year did the bottom water reach the Central Basin as reported in Schauer et al. (2002). This is sensitive to our Novaya Zemlya Bank definition, and expanding the area southward to 72°N yields more south-westward flowing tracers (not shown). Contribution from Central Bank to the BSX comes from two branches (Fig. 10). A northern branch exits the Barents Sea together with a branch from Great Bank, while a southward branch goes into a cyclonic circulation around the Central Basin. The latter was also reported by Ozhigin et al. (2000).

Due to different distances and paths, CDW from the different banks do no reach BSX simultaneously. Analysis of deseasoned monthly data (Fig. 11a) indicates that CDW on Novaya Zemlya Bank mainly reaches BSX within 1-7 months, which is consistent with the estimated time for cascading from this area (Shapiro et al., 2003). The contribution from Great Bank shows highest correlation with the BSX outflow between 1-8 months, whereas water from Central Bank seems to reach BSX within ~1.5 years. Export of CDW in the BSX is thus rather a continuous than a seasonal feature. Significant correlations are also found at larger lags due to remnants on the banks or in the deeper basins. Loeng (1991) suggested that in some periods the Central Basin would gradually fill up with high density water accumulated over several years. Eventually a flushing of the basin could occur. Such flushing events would be in addition to the annual contributions of CDW from the banks, and could result in significant episodic signals in the dense flow leaving the Barents Sea toward the Arctic Ocean.

Part of the CDW formed in the Barents Sea also leaves between Svalbard and Frans Josef Land. The main contributors to this flow are Central Bank and Great Bank (Fig. 10),
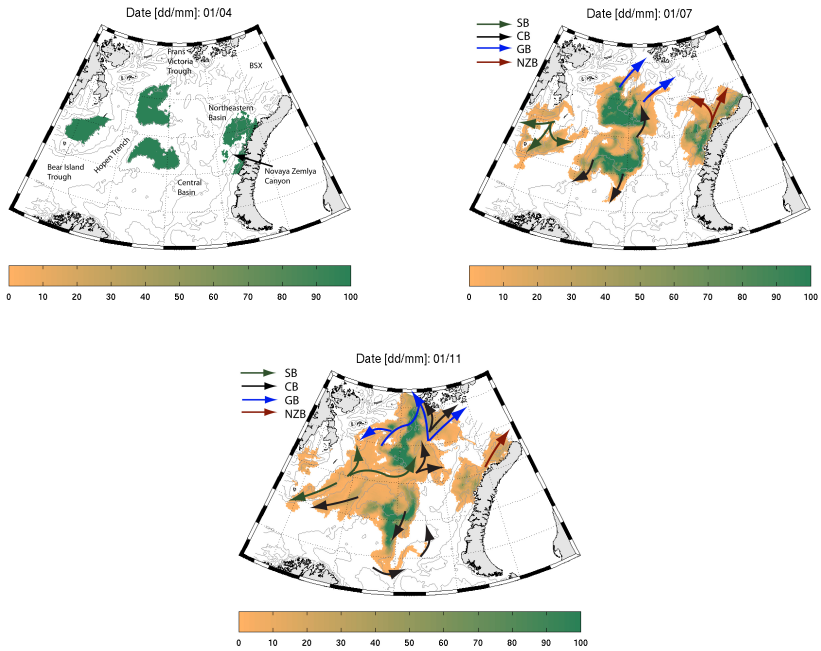
Figure 10: Bottom water circulation during year 2000 calculated using an Eulerian advection model (see details in text). The upper panel shows the initial distribution of the tracer on 1 April, 2000, whereas the middle and bottom panels show the tracer distribution after 3 and 7 months of integration. Concentrations (colorbar) are shown for depths below 50 m.

and maximum correlations between these sources and the outflow are found at lags from 5-6 months (Fig. 11b). The model also indicates that CDW from Spitsbergen Bank leaves in this area, as there is a north-eastward flow which splits into two branches south of Great Bank. This slow northward flow of dense water is supported by Fig. 11b, which shows a significant peak after 21 months.

Outflow of CDW also occur through the western Barents Sea, and both Spitsbergen

31

Bank and Central Bank contribute to this flow (Fig. 10). Most of the Spitsbergen Bank CDW leaves north of Bear Island, but there is also a fraction going to the south of the island. Central Bank contributes with a branch following the rim of the Hopen Trench exiting south of Bear Island in agreement with Quadfasel et al. (1992). This flow reaches the BSO within 7-10 months (not shown).

The branches of bottom water circulation are confirmed by observations (not shown), and are also consistent with the circulation scheme of Aksenov et al. (2010). The colorscale in Fig. 10 is an indicator of mixing showing that dense water on Central Bank and Great Bank is more stationary or less diffused compared to Spitsbergen Bank and Novaya Zemlya Bank.
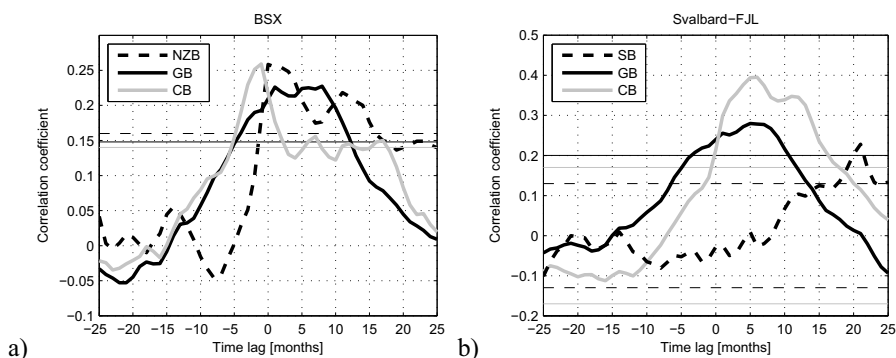

Figure 11: Lagged correlation analysis of CDW export in the northern Barents Sea with respect to CDW volume on the banks. Positive lags indicate that CDW formation on the banks leads the export. Time series have been deseasoned and detrended. Thin lines show the 95% significance levels. Autocorrelation has been taken into account by adjusting the effective number of independent observations.

7. Cold Deep Water export

Dense water formed in Arctic shelf seas influences the water mass properties and thermohaline circulation of the Arctic Ocean (e.g. Nansen, 1906; Aagaard et al., 1985; Jones et al., 1995; Meincke et al., 1997). The majority of the CDW exits the Barents Sea in the BSX where it constitutes 63% (1.2 Sv) of the simulated mean net flow of 1.9 Sv. An additional 0.4 Sv of CDW leaves between Svalbard and Frans Josef Land, making the total contribution of CDW directly from the Barents Sea to the Arctic Ocean 1.6 Sv. In the west, 0.02 Sv leaves between Svalbard and Bear Island, and 0.1 Sv south of Bear Island. The simulated annual mean CDW outflow density at BSX is 1028.07 kg m^{-3} (T=-0.78°C, S=34.91). This density is matched in the Eurasian Basin at around 1000 m (observations from the Environmental Working Group; Swift et al., 2005). Higher densities (>1028.10 kg m^{-3}) in the BSX occur in e.g. 1975-76 and in the late 1980s, and this water would be able to descend to 2000 m depth in the Arctic Ocean. The density variability is mainly determined by salinity (r>0.9), ranging from 34.85 (1028.00 kg m^{-3}) in 1950 to 34.97 (1028.13 kg m^{-3}) in 1988. The latter corresponds to a period of both maximum CDW formation and density on Novaya Zemlya Bank (Fig. 5). The impact of Barents Sea dense water on the intermediate depth waters (between 700 m and 1700 m) of the Arctic Ocean is described by e.g. Rudels et al. (1994) and Schauer et al. (1997). Aagaard et al. (1981) argued that the cold halocline of the Arctic Ocean is maintained by lateral advection of water near the freezing point with a salinity of 34.75 from the surrounding continental shelves. Our results indicate that most of the outflowing water from the Barents Sea is more saline, and thus support the view that the contribution to the Arctic halocline from the Barents Sea is rather supplied by the winter mixed layer (Rudels et al., 1991; Steele et al., 1995; Rudels et al., 2004).

The contribution from the three banks supplying CDW to the flow between Svalbard

and Novaya Zemlya (Central Bank, Great Bank and Novaya Zemlya Bank) is on average 0.52 Sv (Fig. 12). The estimate is possibly larger as renewal rates and entrainment is not considered. Still, covering only ~7% (9% including Spitsbergen Bank) of the total ocean area, these banks on average contribute with approximately 1/3 of the net CDW export from the Barents Sea. The remaining CDW is produced either broadly over the shelf or on banks not considered here (Fig. 12, termed CDW non-banks). Variation in the CDW net flow is mostly governed by variations in CDW non-banks, while the banks produce CDW at a more stable rate. In some periods the relative contribution from the banks is larger due to low amounts of CDW non-banks (early 1960s, the late 1970s and the late 1990s). All CDW time series in Fig. 12 have positive correlation (r=0.62-0.82) between volume flux and density, meaning that during periods of high export the CDW is also denser.

A prominent feature in the CDW transport, related to the CDW non-banks contribution, is multi-year cycles of persistent high/low outflow (Fig. 12). Maximum CDW export during the early 1970s and the late 1980s/early 1990s correspond to relatively warm periods with high inflow through the BSO. The local minimum (late 1970s) occurred during a cold period with low inflow (Fig. 12 and Ingvaldsen et al., 2003; Levitus et al., 2009). Warm periods are characterized by higher salinities (Skagseth et al., 2008; Levitus et al., 2009), lower ice cover (Vinje, 2009) and higher overall heat loss of the AW throughflow (Smedsrud et al., 2010; Årthun and Schrum, 2010), which all favor CDW formation by general cooling of AW. CDW non-banks is strongly linked to the heat loss in the region of the main AW throughflow (Fig. 13). The eastern Barents Sea seems to be a key area with correlation coefficients of 0.6-0.8 and a 15 times increase of CDW transport (from 0.04 to 0.6 Sv) over the region. This area corresponds to the extent of the winter mean 0°C surface isotherm, indicative of the position of the Polar Front and size of cooling area (Smedsrud et al., 2010). Changes in cooling area are associated with changes in ocean heat transport (Smedsrud et al., 2010), driving large interannual heat loss variability west
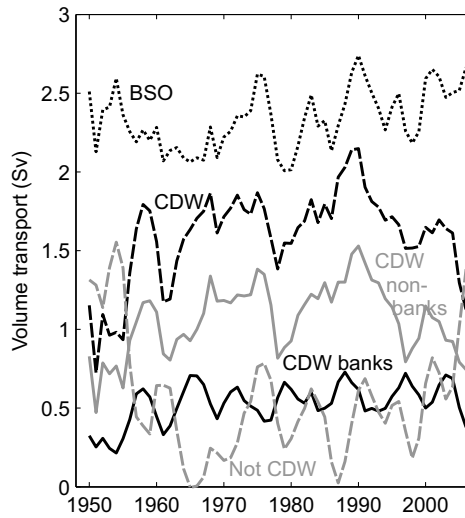
34

Figure 12: Simulated net outflow of CDW (dashed black line) and other water masses (dashed gray line) between Svalbard and Novaya Zemlya. The CDW export is partitioned into CDW formed on the banks (solid black line) and CDW formed broadly over the shelf (CDW non-banks, gray). The net inflow to the Barents Sea in the BSO is also included (dotted black line). All series have been filtered using a 3 year running mean.

of Novaya Zemlya (Årthun and Schrum, 2010). Hence, during warm periods with high throughflow enhanced heat loss in the eastern Barents Sea provides sufficient cooling of AW to produce CDW, and the result is increased export of CDW to the Arctic Ocean. In cold periods the opposite occurs and conditions on the banks and dense water formation by brine rejection become more important (Fig. 12).

Although the net CDW export from the Barents Sea increased by increasing temperatures during the 1970s to the 1990s, it was particularly low during the periods of maximum temperatures in the early 1950s and late 2000s (Fig. 12; Levitus et al., 2009). The last decade has been especially warm with subsurface temperatures in the central Barents Sea
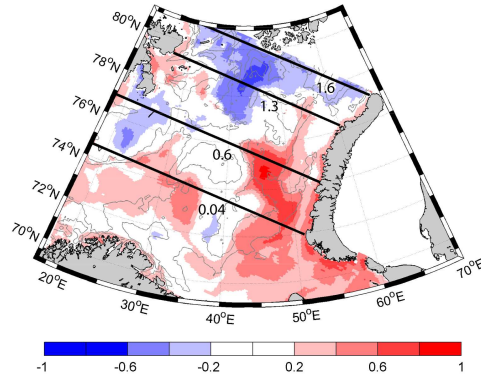
Figure 13: Correlation between annual oceanic heat loss (sensible, latent, and longwave heat fluxes) and net CDW transport (non-banks) between Svalbard and Novaya Zemlya. 200 m and 300 m isobaths are indicated by gray lines. Numbers give net CDW transport through different sections (black lines).

(11-57°E, 69-78°N) of 6.6°C between 2002 and 2006 compared to 4.2°C in 1968-1972 (Levitus et al., 2009). Thus, despite the large oceanic heat loss within the Barents Sea the additional heat in the warmest years can prevent formation of CDW, and export of CDW to the Arctic Ocean is strongly reduced. This result is consistent with the results of Harms (1997) who argued that in warm periods with high AW inflow the CDW production would be reduced, and Backhaus et al. (1997) who proposed that increasing import of warm AW onto the Barents Sea shelf might cause a negative feedback on both deep reaching convection and ice growth. It is also noteworthy that the strong reduction of net CDW export during the extremely warm periods corresponds to an increase in export of water masses having temperatures above 0°C (Fig. 12). This might have a profound impact on the heat transport to the Arctic Ocean.

The volume of CDW from the banks has a negative correlation to the variations in export of waters warmer than 0°C (Fig. 12, r=-0.62 for annual values and r=-0.71 for 3

36

year moving averages). This implies that strong CDW formation on the banks gives less net export of warmer ($T > 0°C$) water from the Barents Sea. When flowing off the banks substantial mixing between CDW and the surrounding water takes place and mixing will also occur en route from the bank to the outflow area. Schauer et al. (2002) explained the relatively high (-0.5°C) observed temperatures in the deeper layers in BSX with substantial mixing between brine-enriched water at the freezing point and AW. Mixing is likely to be most dominant for CDW being close to the warmest AW and/or having the longest transport route, i.e. the CDW flowing southwards from Central Bank (Fig. 10). Mixing will increase the temperature of the CDW, but also decrease the temperature of the surrounding water. Large volumes of CDW on the banks therefore likely results in less export of water warmer than 0°C. Our results indicate that the substantial cooling and water mass transformations occurring on the banks modify the warmer throughflow by downstream mixing. Consequently, CDW formed on the banks acts as a cooler for the AW throughflow and is important also for the net export of waters warmer than 0°C.

From Fig. 13 it is evident that increased heat loss in a narrow band along the southern coast of Novaya Zemlya will increase the volume of CDW non-banks. This area is part of the shallow shelf along Novaya Zemlya, but due to our geographical definition of the bank (Fig. 1 and Tab. 1) CDW formed in this region is classified as CDW non-banks. CDW formation in this region has been documented by earlier studies (Ivanov and Shapiro, 2005). Furthermore, the discrepancy between simulated and observed bottom water temperature and salinity (Fig. 4), and the corresponding sensitivity in CDW formation to a corrected local water mass definition (Sec. 4.5) can influence the relative strength of the different outflows. For instance, colder and more saline bottom waters on Great Bank could imply a potential overestimation of CDW export between Svalbard and Frans Josef Land. Limited measurements of dense water transports exist for the northern Barents Sea, although the characteristics of the outflow through the Victoria Channel have been discussed by Rudels

(1986), Schauer et al. (1997) and Rudels and Friedrich (2000). The simulated net through-flow between Svalbard and Frans Josef Land is 0.3 Sv (outflow), in close agreement with Maslowski et al. (2004, 0.36 Sv) and Aksenov et al. (2010, 0.4 Sv).

8. Summary and Conclusions

Previously unpublished hydrographic observations during late summer (August-October 1970-2007) demonstrate substantial interannual variability in dense water properties on shallow banks in the Barents Sea (Spitsbergen Bank, Central Bank, Great Bank, Novaya Zemlya Bank). Between 1970 and 2007 the mean bottom water temperature on Novaya Zemlya Bank varied by 2.0°C, while the salinity variation was 0.44. The temperature and salinity ranges on Spitsbergen Bank were even larger; 5.1°C and 1.07, respectively. These waters condition the intermediate waters of the Arctic Ocean (e.g. Rudels et al., 1994), and understanding the variability and processes involved are therefore of great interest.

To investigate formation of dense Cold Deep Water (CDW: $T<0$°C and $S>34.75$) and processes important to its interannual variability, a new and improved setup of the regional coupled ice-ocean model HAMSOM (Hamburg Shelf Ocean Model) was applied to the Barents Sea for the period 1948 to 2007. An advection algorithm was also applied to elucidate the paths of dense water within the Barents Sea. The model identifies several distinct branches, which has implications for the residence time of dense water and thus mixing with ambient waters en route to the outflow areas.

The main findings from our study are:

(1) CDW variability on Spitsbergen Bank and Central Bank is associated with advection of Atlantic Water, which modifies the initial (November) surface salinity and oceanic heat loss. The high salinities on Central Bank imply that atmospheric cooling is enough to produce CDW, but initial salinities have a strong influence through the

effect on water column stability. Strong tidal currents also influence heat loss and salt input on Spitsbergen Bank. CDW anomalies on Great Bank and Novaya Zemlya Bank are also related to the initial salinity which is affected by ice import from the Arctic Ocean and the fresh Novaya Zemlya Coastal Current, respectively. Novaya Zemlya Bank has the highest salt input from ice growth during winter ($\sim$0.2 kg m^{-2} day^{-1}) and variations in ice extent are important for dense water temperatures and salinities.

(2) The main net CDW export is between Frans Josef Land and Novaya Zemlya (1.2 Sv). Part of the CDW also exits the Barents Sea to the Arctic Ocean between Svalbard and Frans Josef Land (0.4 Sv), whereas smaller amounts exit into the Norwegian Sea. The mean density of the outflowing CDW north of Novaya Zemlya is 1028.07 kg m^{-3}, which compares to observed densities below 1000 m in the Arctic Ocean. Compared to the total outflow 1/3 of the CDW originates from the banks, which represent 9% of the Barents Sea area. During cold periods with reduced AW inflow conditions on the banks become more important and dense water formation by brine rejection plays a larger role. Strong CDW formation on the banks also gives less net export of warmer water (T>0°C) from the Barents Sea, suggesting that water mass transformations occurring on the banks modify the warmer throughflow by downstream mixing.

(3) Cooling of northward flowing Atlantic Water and general ice growth in the northern Barents Sea is the most important driver of CDW formation, and therefore also CDW export to the Arctic Ocean. The dense outflow into the Arctic Ocean displays large interannual and quasi-decadal variability, corresponding with variations in the Atlantic Water inflow. Warm periods tend to have high Atlantic inflow, a larger heat loss to the atmosphere, and high CDW export.

We have found that the Barents sea produces and exports CDW effectively for a large

range of forcing, sending ~70% of the shallow inflowing water to depths below 1000 m in the Arctic Ocean. However, the last ten years have been anomalously warm, both in the world oceans in general and in the Barents Sea. This recent warming has decreased the CDW production and export. While this might suggest a general shift due to a gradual global warming, the recent warming has similar characteristics to a warm period in the 1950s. Future observations of the Atlantic inflow and dense outflow should remain a high priority to follow the ongoing changes, and determine whether the Barents Sea will return to a colder state once again. What now seems to be clear is that the banks in the Barents Sea are very steady contributors to the CDW production, and may thus turn out to be even more important in the future.

Acknowledgments

References

Aagaard, K., Coachman, L. K., Carmack, E., 1981. On the halocline of the Arctic Ocean. Deep-Sea Res. Part A. 28, 529–545.

Aagaard, K., Swift, J. H., Carmack, E. C., 1985. Thermohaline circulation in the Arctic Mediterranean seas. J. Geophys. Res. 90 (NC3), 4833–4846.

Ådlandsvik, B., Loeng, H., 1991. A study of the climatic system in the Barents Sea. Polar Res. 10, 45–49.

Aksenov, Y., Bacon, S., Coward, A. C., Nurser, A. J. G., 2010. The North Atlantic inflow to the Arctic Ocean: High-resolution model study. J. Mar. Syst. 79 (1-2), 1–22.

Anderson, L. G., Jones, E. P., Lindegren, R., Rudels, B., Sehlstedt, P. I., 1988. Nutrient regeneration in cold, high salinity bottom water of the Arctic shelves. Cont. Shelf Res. 8 (12), 1345–1355.

Årthun, M., Schrum, C., 2010. Ocean surface heat flux variability in the Barents Sea. J. Mar. Syst. 83, 88–98.

Backhaus, J. O., Fohrmann, H., Kampf, J., Rubino, A., 1997. Formation and export of water masses produced in Arctic shelf polynyas - Process studies of oceanic convection. ICES J. Mar. Sci. 54 (3), 366–382.

Barthel, K., Daewel, U., Pushpadas, D., Schrum, C., Svendsen, S. W., Wehde, H., Årthun, M., 2011. Resolving frontal structures: On the computational costs and pay-off using a less diffusive but computational more expensive advection scheme , In prep.

Bleck, R., 1998. Ocean modeling in isopycnic coordinates. In: Ocean modeling and parameterization. Kluwer Academic Publishers, pp. 423–448.

Blindheim, J., 1989. Cascading of Barents Sea bottom water into the Norwegian Sea. Rapports et Procéss-verbaux des Réunions du Conseil International par l'Exploration de la Mer 188, 49–58.

Cavalieri, D., Parkinson, C., Gloersen, P., Zwally, H. J., 1996, updated 2008. Sea ice concentrations from Nimbus-7 SMMR and DMSP SSM/I passive microwave data. Digital media, National Snow and Ice Data Center, Boulder, Colorado.

Cavalieri, D. J., Martin, S., 1994. The contribution of Alaskan, Siberian, and Canadian coastal polynyas to the cold halocline layer of the Arctic Ocean. J. Geophys. Res. 99 (C9), 18343–18362.

Ellingsen, I., Slagstad, D., Sundfjord, A., 2009. Modification of water masses in the Barents Sea and its coupling to ice dynamics: a model study. Ocean Dyn. 59 (6, Sp. Iss. SI), 1095–1108.

Francis, J. A., Hunter, E., 2007. Drivers of declining sea ice in the Arctic winter: A tale of two seas. Geophys. Res. Lett. 34 (17).

Gammelsrød, T., Leikvin, Ø., Lien, V., Budgell, W. P., Loeng, H., Maslowski, W., 2009. Mass and heat transports in the NE Barents Sea: Observations and models. J. Mar. Syst. 75, 56–69.

Gerdes, R., Schauer, U., 1997. Large-scale circulation and water mass distribution in the Arctic Ocean from model results and observations. J. Geophys. Res. 102 (C4), 8467–8483.

Golubev, V. A., Zuyev, A. N., 1999. Barents and Kara Seas Oceanograhic Database (BarKode). Tech. Rep. ACSYS IACPO Report 5, World Research Program, Arctic Climate System Study, Tromsø, Norway.

Häkkinen, S., Cavalieri, D. J., 1989. A study of oceanic surface heat fluxes in the Greenland, Norwegian, and Barents Sea. J. Geophys. Res. 94, 6145–6157.

Harms, I. H., 1997. Water mass transformation in the Barents sea - Application of the Hamburg Shelf Ocean Model (HamSOM). ICES J. Mar. Sci. 54 (3), 351–365.

Harms, I. H., Schrum, C., Hatten, K., 2005. Numerical sensitivity studies on the variability of climate-relevant processes in the Barents Sea. J. Geophys. Res. 110, C06002.

Hibler, W. D., 1979. A dynamic thermodynamic sea-ice model. J. Phys. Oceanogr. 9 (4), 815–846.

Ingvaldsen, R., Loeng, H., Ådlandsvik, B., 2003. Climate variability in the Barents Sea during the 20th century with focus on the 1990s. ICES Mar. Sci. Symp. 219, 160–168.

Ingvaldsen, R., Loeng, H., Asplin, L., 2002. Variability in the Atlantic inflow to the Barents Sea based on a one-year time series from moored current meters. Cont. Shelf Res. 22, 505–519.

Ivanov, V. V., Shapiro, G. I., 2005. Formation of a dense water cascade in the marginal ice zone in the Barents Sea. Deep-Sea Res. Part 1. 52 (9), 1699–1717.

Ivanov, V. V., Shapiro, G. I., Huthnance, J. M., Aleynik, D. L., Golovin, P. N., 2004. Cascades of dense water around the world ocean. Prog. Oceanogr. 60 (1), 47–98.

Jones, E. P., Rudels, B., Anderson, L. G., 1995. Deep waters of the Arctic Ocean - Origins and circulation. Deep-Sea Res. Part 1. 42 (5), 737–760.

Kalnay, E., Kanamitsu, M., Kistler, R., Collins, W., Deaven, D., Gandin, L., Iredell, M., Saha, S., White, G., Woollen, J., Zhu, Y., Chelliah, M., Ebisuzaki, W., Higgins, W., Janowiak, J., Mo, K. C., Ropelewski, C., Wang, J., Leetmaa, A., Reynolds, R., Jenne, R., Joseph, D., 1996. The NCEP/NCAR 40-year reanalysis project. Bull. Am. Met. Soc. 77, 437–471.

Killworth, P. D., 1983. Deep convection in the world ocean. Rev. Geophys. 21 (1), 1–26.

Knipowitsch, N., 1905. Hydrologische untersuchungen im Europäischen Eismeer. Ann. Hydro. Mar. Met. 33, 241–260.

Koentopp, M., Eisen, O.and Kottmeier, C., Padman, L., Lemke, P., 2005. Influence of tides on sea ice in the Weddell Sea: Investigations with a high-resolution dynamic-thermodynamic sea ice model. J. Geophys. Res. 110 (C2).

Kowalik, Z., Proshutinsky, A. Y., 1994. The Arctic Ocean tides. In: The Polar Regions and Their Role in Shaping the Global Environment. Vol. 85 of Geophysical Monograph. American Geophysical Union, pp. 137–158.

Kvingedal, B., 2005. Sea-ice extent and variability in the Nordic Seas, 1967-2002. In: The Nordic Seas: An Integrated Perspective. Vol. 158 of Geophysical Monograph. American Geophysical Union, pp. 137–156.

Kwok, R., 2009. Outflow of Arctic Ocean sea ice into the Greenland and Barents Seas: 1979-2007. J. Clim. 22 (9), 2438–2457.

Lammers, R. B., Shiklomanov, A. I., 2000. R-ArcticNet, A Regional Hydrographic Data Network for the Pan-Arctic Region. Tech. rep., Water Systems Analysis Group, University of New Hampshire, Durham, NH, data available at http://www.r-arcticnet.sr.unh.edu/v4.0/index.html.

Leppäranta, M., Zhang, Z. H., 1992. A viscous-plastic ice dynamic test model for the Baltic Sea. Int rep pp 14, Finnish Institute of Marine Resources.

Levitus, S., Matishov, G., Seidov, D., Smolyar, I., 2009. Barents Sea multidecadal variability. Geophys. Res. Lett. 36.

Loeng, H., 1991. Features of the physical oceanographic conditions of the Barents Sea. Polar Res. 10 (1), 5–18.

Loeng, H., Sagen, H., Ådlandsvik, B., Ozighin, V., 1993. Current measurements between Novaya Zemlya and Frans Josef Land, September 1991-September 1992. Institute of

Marine Research, Norway. Department of Marine Environment, Report 2/1993, pp 23 + 4 appendices.

Marsland, S. J., Haak, H., Jungclaus, J. H., Latif, M., Roske, F., 2003. The Max-Planck-Institute global ocean/sea ice model with orthogonal curvilinear coordinates. Ocean Model. 5 (2), 91–127.

Martin, S., Cavalieri, D. J., 1989. Contributions of the Siberian shelf polynyas to the Arctic Ocean intermediate and deep water. J. Geophys. Res. 94 (C9), 12725–12738.

Maslowski, W., Marble, D., Walczowski, W., Schauer, U., Clement, J. L., Semtner, A. J., 2004. On climatological mass, heat, and salt transport through the Barents Sea and Fram Strait from a pan-Arctic coupled ice-ocean model simulation. J. Geophys. Res. 109, C03032.

Maus, S., 2003. Interannual variability of dense shelf water salinities in the north-western Barents Sea. Polar Res. 22 (1), 59–66.

Meincke, J., Rudels, B., Friedrich, H. J., 1997. The Arctic Ocean Nordic Seas thermohaline system. ICES J. Mar. Sci. 54 (3), 283–299.

Midttun, L., 1985. Formation of dense bottom water in the Barents Sea. Deep-Sea Res. Part A. 32 (10), 1233–1241.

Mosby, H., 1938. Svalbard Waters. Geofysiske Publikasjoner 12 (4), 1–85.

Nansen, F., 1906. Northern waters: Captain Roald Amundsen's oceanographic observations in the Arctic Seas in 1901. Vol. 3. Videnskabs-Selskabets Skrifter, I, Matematisk-Naturv. Klasse.

Nilsen, J. E. Ø., Hátún, H., Mork, K. A., Valdimarsson, H., 2008. The NISE Dataset. Tech. Rep. 08-01, Faroese Fisheries Laboratory.

Ozhigin, V. K., Trofimov, A. G., Ivshin, V. A., 2000. The Eastern Basin Water and currents in the Barents Sea. In: ICES C.M. 2000/L:14. p. 19.

Padman, L., Erofeeva, S., 2004. A barotropic inverse tidal model for the Arctic Ocean. Geophys. Res. Lett. 31 (2).

Parsons, A. R., 1995. On the Barents Sea polar front in summer and interpretations of the associated regional oceanography using an Arctic Ocean general circulation model. Ph.D. thesis, Nav. Postgrad. Sch., Monterey, Calif.

Pfirman, S. L., Bauch, D., Gammelsrød, T., 1994. The Northern Barents Sea: Water mass distribution and modification. In: The Polar Regions and Their Role in Shaping the Global Environment. Vol. 85 of Geophysical Monograph. American Geophysical Union, pp. 77–94.

Quadfasel, D., Rudels, B., Kurz, K., 1988. Outflow of dense water from a Svalbard fjord into the Fram Strait. Deep-Sea Res.Part A 35 (7), 1143–1150.

Quadfasel, D., Rudels, B., Selchow, S., 1992. The Central Bank vortex in the Barents Sea: watermass transformation and circulation. ICES Mar. Sci. Symp. 195, 40–51.

Rudels, B., 1986. The θ-S relations in the Northern Seas: Implications for the deep circulation. Polar Res. 4 (2), 133–159.

Rudels, B., 1987. On the mass balance of the Polar Ocean, with special emphasis on the Fram Strait. Nor. Polarinst. Skr. 188.

Rudels, B., Jones, E. P., Anderson, L. G., Kattner, G., 1994. On the intermediate depth waters of the Arctic Ocean. In: O. M. Johannesen, R. D. Muench and J. E. Overland (Ed.), The Polar oceans and their role in shaping the global environment. AGU Geophysical Monographs, 85, pp. 33–46.

Rudels, B., Friedrich, H. J., 2000. The transformations of Atlantic Water in the Arctic Ocean and their significance for the freshwater budget. In: E. L. Lewis et al. (Ed.), The freshwater budget of the Arctic Ocean. Kluwer Academic Publishers, pp. 503–532.

Rudels, B., Jones, E. P., Schauer, U., Eriksson, P., 2004. Atlantic sources of the Arctic Ocean surface and halocline waters. Polar Res. 23 (2), 181–208.

Rudels, B., Larsson, A. M., Sehlstedt, P. I., 1991. Stratification and water mass formation in the Arctic Ocean - some implications for the nutrient distribution. Polar Res. 10 (1), 19–31.

Sandø, A. B., Gao, Y., Nilsen, J. E. Ø., Lohmann, K., 2010. Importance of heat transports and local air-sea heat fluxes for Barents Sea climate variability. J. Geophys. Res. 115 (C7).

Schauer, U., 1995. The release of brine-enriched shelf water from Storfjord into the Norwegian Sea. J. Geophys. Res. 100 (C8), 16015–16028.

Schauer, U., Loeng, H., Rudels, B., Ozhigin, V. K., Dieck, W., 2002. Atlantic water flow through the Barents and Kara Sea. Deep-Sea Res. Part 1. 49, 2281–2298.

Schauer, U., Muench, R. D., Rudels, B., Timokhov, L., 1997. Impact of eastern Arctic shelf waters on the Nansen Basin intermediate layers. J. Geophys. Res. 102 (C2), 3371–3382.

Schrum, C., Backhaus, J. O., 1999. Sensitivity of atmosphere-ocean heat exchange and heat content in the North Sea and the Baltic Sea. Tellus 51 (4), 526–549.

Schrum, C., Harms, I. H., Hatten, K., 2005. Modelling air-sea exchange in the Barents Sea by using a coupled regional ice-ocean model. Evaluation of modelling strategies. Meteorol. Z. 14 (6), 801–808.

Schrum, C., St. John, M., Alekseeva, I., 2006. ECOSMO, a coupled ecosystem model of the North Sea and Baltic Sea: Part II. Spatial-seasonal characteristics in the North Sea as revealed by EOF analysis. J. Mar. Syst. 61 (1-2), 100–113.

Shapiro, G. I., Huthnance, J. M., Ivanov, V. V., 2003. Dense water cascading off the continental shelf. J. Geophys. Res. 108 (C12).

Simonsen, K., Haugan, P. M., 1996. Heat budgets of the Arctic Mediterranean and sea surface heat flux parameterizations for the Nordic Seas. J. Geophys. Res. 101, 6553–6576.

Skagseth, Ø., 2008. Recirculation of Atlantic Water in the western Barents Sea. Geophys. Res. Lett. 35, L11606.

Skagseth, Ø., Drinkwater, K., Terrile, E., 2011. Wind and buoyancy induced transport of the Norwegian Coastal Current in the Barents Sea, Submitted to J. Geophys. Res.

Skagseth, Ø., Furevik, T., Ingvaldsen, R., Loeng, H., Mork, K. A., Orvik, K. A., Ozhigin, V., 2008. Volume and heat transports to the Arctic Ocean via the Norwegian and Barents Seas. In: Dickson, R., Meincke, J., Rhines, P. (Eds.), Arctic Subarctic Ocean Fluxes: Defining the Role of the Northern Seas in Climate. Springer, New York, pp. 45–64.

Skogseth, R., Haugan, P. M., Haarpaintner, J., 2004. Ice and brine production in Storfjorden from four winters of satellite and in situ observations and modeling. J. Geophys. Res. 109 (C10).

Skogseth, R., Haugan, P. M., Jakobsson, M., 2005. Watermass transformations in Storfjorden. Cont. Shelf Res. 25 (5-6), 667–695.

Smedsrud, L. H., Ingvaldsen, R., Nilsen, J. E. Ø., Skagseth, Ø., 2010. Heat in the Barents Sea: Transport, storage, and surface fluxes. Ocean Sci. 6, 219–234.

Smith, S. R., Legler, D. M., Verzone, K. V., 2001. Quantifying uncertainties in NCEP reanalyses using high-quality research vessel observations. J. Clim. 14 (20), 4062–4072.

Steele, M., Morison, J. H., Curtin, T. B., 1995. Halocline water formation in the Barents Sea. J. Geophys. Res. 100 (C1), 881–894.

Sundfjord, A., Ellingsen, I., Slagstad, D., Svendsen, H., 2008. Vertical mixing in the marginal ice zone of the northern Barents Sea - Results from numerical model experiments. Deep-Sea Res. Part 2 55 (20-21), 2154–2168.

Sweby, P. K., 1984. High resolution schemes using flux limiters for hyperbolic conservation laws. SIAM J. Numer. Anal. 21 (5), 995–1011.

Swift, J. H., Aagaard, K., Timokhov, L., Nikiforov, E. G., 2005. Long-term variability of Arctic Ocean waters: Evidence from a reanalysis of the EWG data set. J. Geophys. Res. 110 (C3).

Vinje, T., 2009. Sea-ice. In: Sakshaug, E., Kovacs, K., Johnsen, G. (Eds.), Ecosystem Barents Sea. Tapir Academic Press, Trondheim, Norway, pp. 65–82.

Winsor, P., Björk, G., 2000. Polynya activity in the Arctic Ocean from 1958 to 1997. J. Geophys. Res. 105 (C4), 8789–8803.

Zhang, X., Zhang, J., 2001. Heat and freshwater budgets and pathways in the Arctic Mediterranean in a coupled ocean/sea-ice model. J. Oceanogr. 57, 207–234.